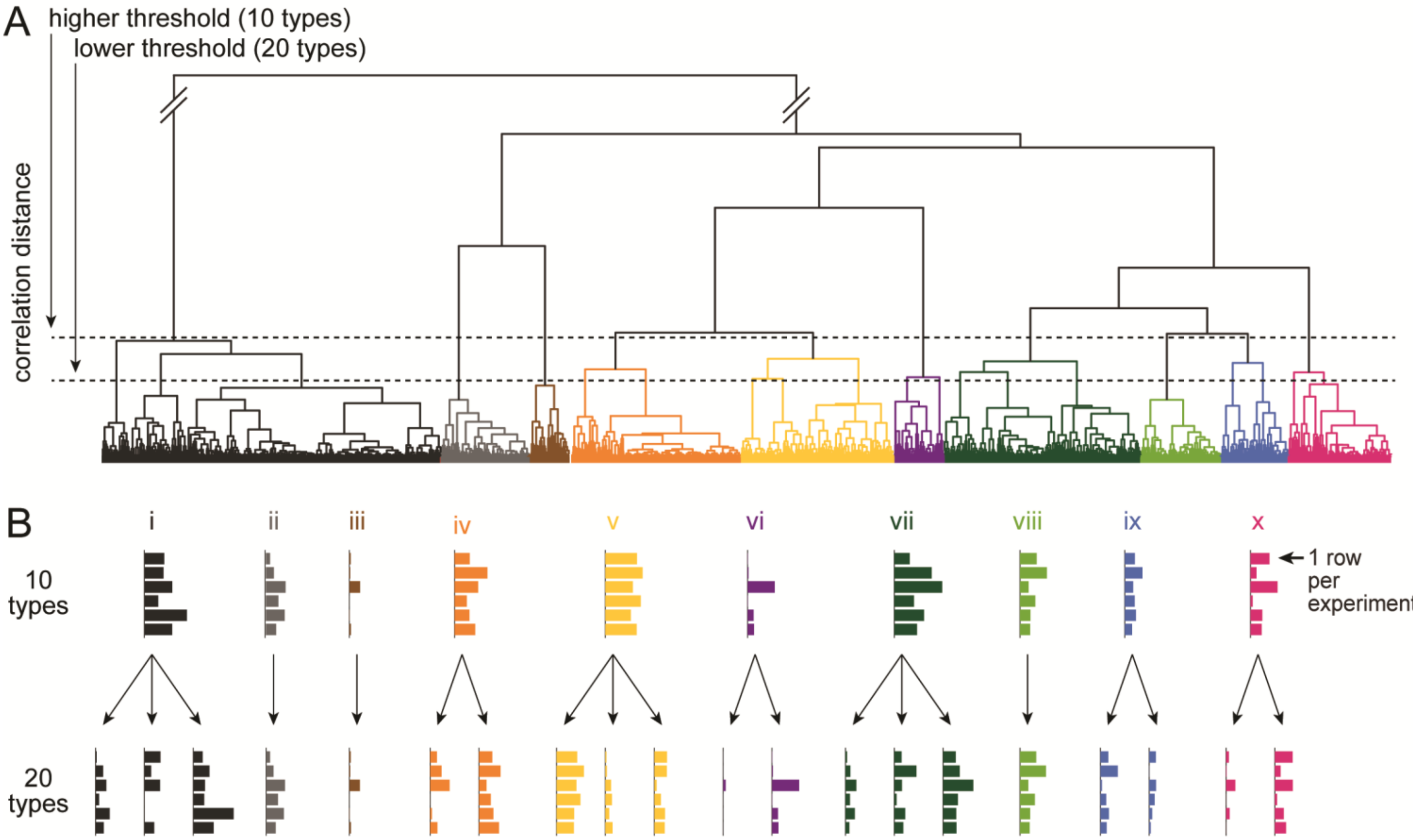

Figure S1. Splitting functional types more finely reduces experiment-to-experiment consistency. Related to Figure 2.

A) Functional clustering of the JON dataset, reproduced from Figure 2A, but now with two thresholds indicated. The higher threshold (k=10 types) was used in Figure 2A, and the colors in the dendrogram represent the 10 JON response types that result from that threshold. The lower threshold (k=20 types) is shown here for illustrative purposes, as an example of how JON types might be split more finely.

B) Pixel counts for 10 types (top) and 20 types (bottom). Each bar shows the number of pixels belonging to a given response type, with each row representing a different experiment in a fly where GCaMP6f was expressed under the control of *nan-Gal4* (n=6). Note that when pixels are split into 20 types, many types appear in only a subset of experiments. For example, splitting type i results in three new types, two of which are found in only some experiments. Bars are normalized within each type; thus, bars colored the same way are represented in the same scale.

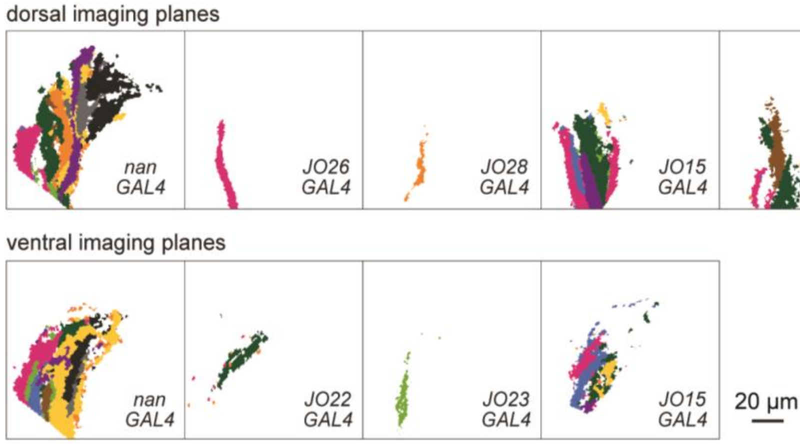

Figure S2. JON types appear at consistent locations in both broad and sparse imaging experiments. Related to Figure 2.
Maps of JON response types in the AMMC. GCaMP6f was expressed under the control of a pan-JON Gal4 line, *nan-Gal4*, or else a Gal4 line targeting a small subset of JONs. One representative experiment is shown for each genotype. Maps depict either a dorsal imaging plane (top row) or a ventral imaging plane (bottom row), or both, depending on which plane(s) captured the response type in question. Note that the spatial location of each response type in the sparse genotypes was consistent with its location in *nan-Gal4* experiments. Note also that the response types which were most difficult to identify consistently in *nan-Gal4* experiments (types iii and vi) appeared in sparse Gal4 lines at the same locations where they appeared in nan-Gal4 experiments: type iii appears in JO2, and type vi appears in JO29.

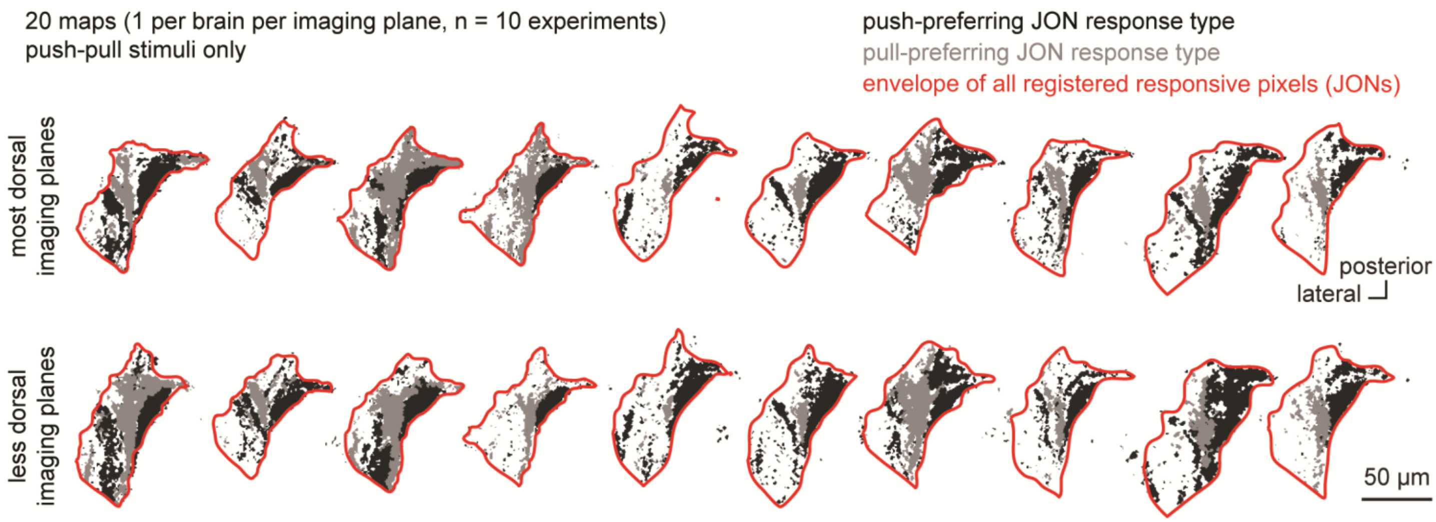

Figure S3. Maps of JON responses to push and pull stimuli in the AMMC. Related to Figure 2 and Figure 3.

GCaMP6f was expressed under the control of *nan-Gal4* (n=10). Pixels were selected if they showed significant modulation in response to push or pull stimuli only. Pixels were then divided into two functional types. As one would expect, the two types resembled type i (push) and type ii (pull) shown in Figure 2 and Figure 3, both in terms of their functional tuning properties and their spatial location. Pixels belonging to the two types are shown in black and gray, respectively. Two dorsal planes are represented for each experiment, one being more dorsal than the other. The outline represents the envelope of the entire JON axon bundle (all pixels that responded significantly to any vibration stimulus or push-pull stimulus), and is intended to highlight the relative location of push- and pull- preferring types in the bundle. Note that responses to steady displacements (push-pull stimuli) were predominant in the most medial part of the JON bundle. Pull-preferring subregions were immediately adjacent to push-preferring subregions, with pull- subregions typically found lateral-posterior to push subregions. Instances of directionally selective responses (to either push or pull stimuli) were consistently found in the lateral part of the bundle as well.

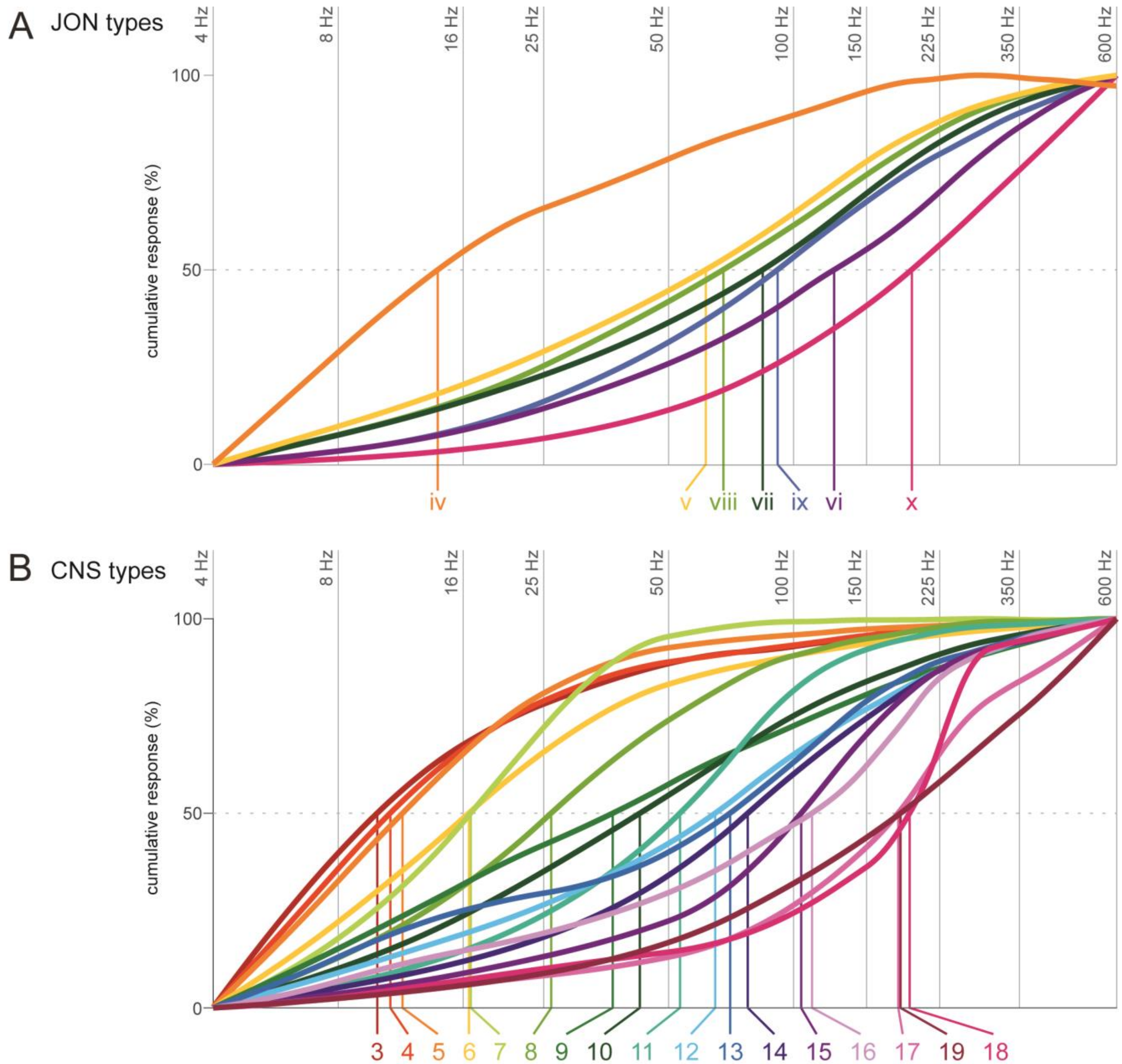

Figure S4. Identifying the "center frequency" of each response type. Related to Figure 3, Figure 5, and Figure 6.

Plots show frequency tuning curves transformed into cumulative response functions for JON (A) and CNS types (B). Here, the cumulative response at each vibration frequency is the summed response at all preceding (lower) log-interpolated frequencies, normalized to the cumulative maximum. Frequency tuning data are from Figure 3B (JONs) and Figure 5B (CNS). Vertical lines denote the "center frequency" for each response type. This is the frequency corresponding to the 50% level of the cumulative response function. In essence, the center frequency is the center of mass of the frequency tuning curve. The center frequency is often close to the frequency that elicits the peak response; however, if the frequency tuning curve is skewed, then the center frequency will reflect this skew. These plots omit the response types that respond best to steady displacements (JON-i/JON-ii, CNS-1/CNS-2), as well as the JON type that is inhibited by all stimuli (JON-iii). JON and CNS types are colored with a rainbow color scheme, where red-orange corresponds to lowest center frequencies and purple-violet corresponds to highest center frequencies. CNS type names and colors are ordered by center frequency (except for type 19, which was assigned the last place in the naming scheme because the response of this type grows monotonically with vibration frequency and appears to be non-saturated). Note that JON type names follow the dendrogram order from Figure 2, and only their colors are sorted according to frequency.

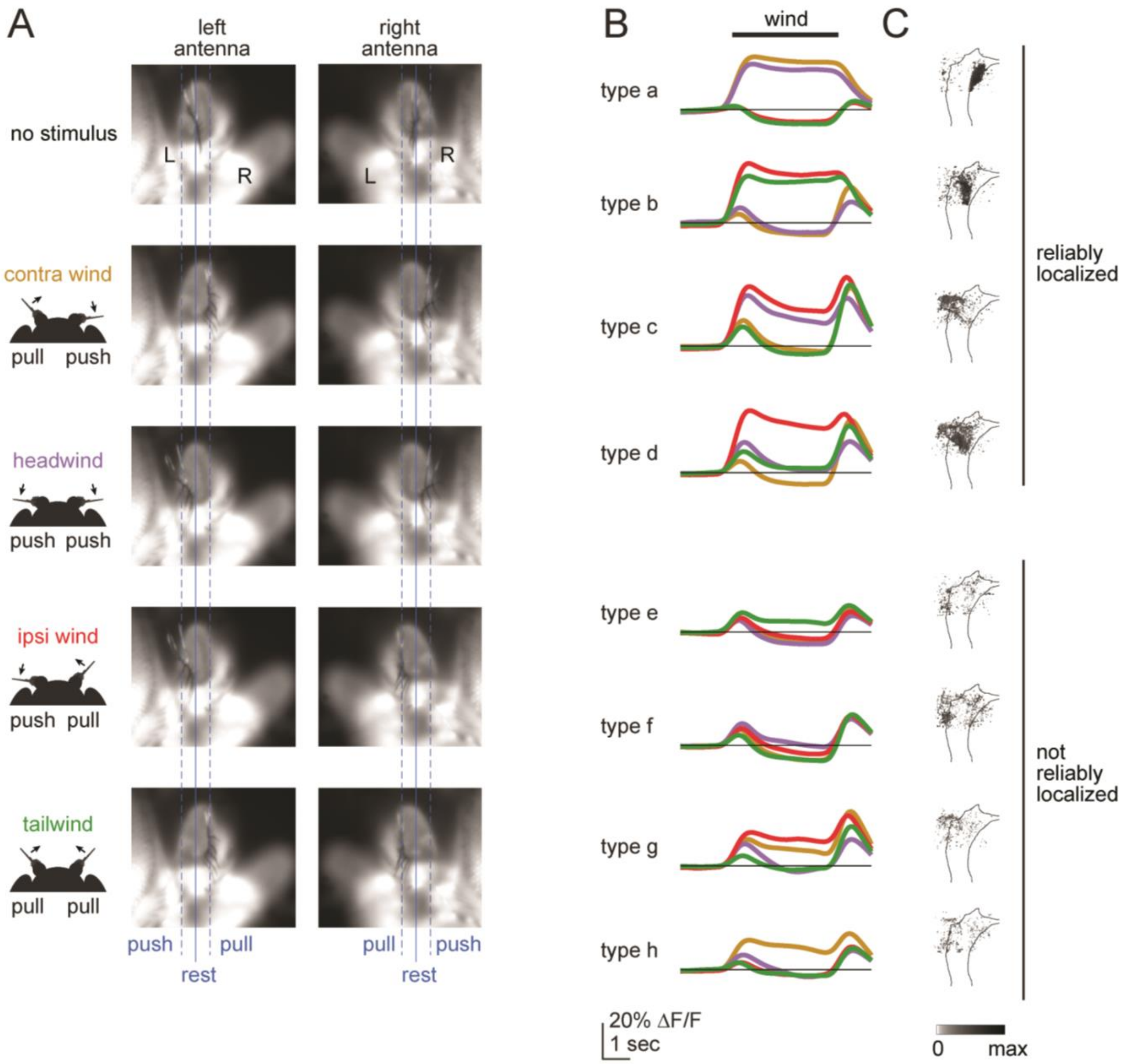

Figure S5. Antennal and neural responses to wind. Related to Figure 7.
A) Images of both antennae in each stimulus configuration. The head is upside down. The left and right images were captured with a pair of cameras, with each camera pointing down the long axis of one arista. The vertical lines are intended to facilitate comparisons between images.
B) Pixels from four experiments were divided into eight functional types, based on responses to the wind stimuli only. Four response types (types a-d) are shown in Figure 7B. Here we show response dynamics for all eight functional types. Types a-d responded robustly to one or two of the wind stimuli, whereas types e-h responded more weakly; types e-h were therefore omitted from Figure 7B.
C) Maps of each type at a *z*-level near the center of the JON axon bundle. Gray scale maps represent the proportion of responsive pixels assigned to the corresponding type across all sampled z levels. The outline represents the envelope of the JON axon bundle at a particular *z*-level. Note that types a-c localized to discrete and consistent regions of the brain, whereas types e-h did not.